Research Article

Edge detection and magnetic basement depth of Danko area, northwestern Nigeria, from low-latitude aeromagnetic anomaly data

Naheem Banji Salawu[1] · **Saminu Olatunji**[2] · **Leke Sunday Adebiyi**[3] · **Nurudeen Kolawole Olasunkanmi**[4] · **Silas Sunday Dada**[5]

Abstract

This study aims at estimating depths and boundaries of magnetic source bodies, in order to provide an indirect insight into subsurface geologic features within Danko area of Kebbi state. The study area is located within low magnetic latitude. Hence, the total magnetic intensity anomaly map was reduced to the magnetic equator. This is to center magnetic anomalies over their respective magnetic source bodies, which equally makes the interpretation of sources easier. Matched filtering of the reduced-to-equator (RTE) magnetic anomaly map indicates that the anomalies could be represented by two equivalent layers with some additional noise. The estimated mean depths of burial for the regional and residual sources are 1000 m and 500 m, respectively. Horizontal gradient magnitude and tilt derivative methods carried out on the RTE aeromagnetic anomaly map facilitated the identification of two distinct geologic trends bounded by a prominent fault suspected to be the documented Yelwa fault. Furthermore, the analytic signal map showed magnetic basement depth values between 50 and 900 m with an average value of 475 m, indicating a compelling alignment of results with the 500 m depth value for the residual matched filter layer. Several mineral occurrences have been found within the outcropping basement rocks of the study area. Hence, the combined appraisal of source edge locations and magnetic basement depth estimates offers useful information of the underlying basement configuration, which is highly essential for mineral exploration targets that are mostly obscured by regolith cover.

Keywords Danko area · Horizontal gradient magnitude · Tilt derivative · Analytic signal

✉ Naheem Banji Salawu, salawubanji@yahoo.com | [1]BS Geophysical and Consultancy Ltd., Ilorin, Nigeria. [2]Department of Geophysics, University of Ilorin, Ilorin, Nigeria. [3]Department of Physical Sciences, Landmark University, Omu-Aran, Nigeria. [4]Department of Physics and Material Science, Kwara State University, Malete, Nigeria. [5]Department of Geology and Mineral Sciences, Al-Hikmah University, Ilorin, Nigeria.

SN Applied Sciences (2019) 1:1056 | https://doi.org/10.1007/s42452-019-1090-3

Received: 22 March 2019 / Accepted: 13 August 2019 / Published online: 20 August 2019

1 Introduction

Aeromagnetic surveys have been used effectively to investigate the subsurface geology in a wide range of earth science applications, including geothermal, hydrological, archeological, hydrocarbon and mineral studies [1, 2]. In mineral resources, it is a primary tool for evaluating mineral potential in the shallow subsurface when the surface geology is obscured or unrelated to the mineral-bearing rocks beneath. Rocks have different magnetic properties and will create local or regional disturbances (anomalies) in earth's magnetic field. Measurement of the earth's magnetic field can help to model the magnetic properties, in order to estimate depths of the corresponding rocks (magnetic source bodies) and infer shapes (geologic structures) such as faults, folds and contacts between rocks of differing magnetic properties which helps many earth science disciplines including mineral assessments. These magnetic measurements are generally presented in the form of gridded magnetic maps constituting anomalies of interest that are generated from magnetic rocks with various geometries, situated at different depths [3]. Central to the interpretation of aeromagnetic data is the mapping of geologic structures and estimating the depths to magnetic basement underneath the regolith materials, because mineral deposits are more likely to be associated with magnetic basement than with the overlying regolith material. Therefore, depth to magnetic basement is an important element for mineral exploration in regions of unexposed bedrocks. The recent acquisition of high-resolution aeromagnetic data over the entire country of Nigeria has highlighted the importance of magnetic basement map [4], especially in relation to mineral exploration.

Various techniques, based on the frequency analysis of the magnetic field, have been established to define parameters such as location of boundaries and depths of the magnetic rocks that cause anomalies in the magnetic field [5]. The horizontal gradient magnitude is one of such methods used for locating contacts and faults from magnetic anomaly data [6–9]. Other methods for location of source boundaries and depth estimates include analytic signal [10, 11] and tilt derivative [12, 13]. The analysis of aeromagnetic data using derivatives methods is to provide an indirect means of seeing the subsurface by sensing various magnetic properties of rocks. This is to expose hidden tectonic structures essential for solid mineral and hydrocarbon resources, and subsurface water reservoirs. Hence, these methods are consistently utilized to interpret aeromagnetic anomaly data to obtain necessary information for mineral exploration [14].

The Danko area, which is the focus for this study, has not received much geologic attention. Omaru [15] investigated the geologic framework of Danko region by identifying rock units and lineaments using a combination of geologic field work and remote sensing. Binta et al. [16] examined samples of manganese ore collected from dug pit by local artisanal miners for concentration test, in order to determine the mineral potential of the region. These two studies suggest mineral potential in the region, and examination of aeromagnetic data of the study area would help focus future investigations by identifying magnetic source bodies buried beneath the surface.

In this study, we examine the aeromagnetic anomaly data and attempt to identify subsurface geologic structures that may be important in future mineral exploration. We use derivative-based and match filtering methods to identify source depths, edges and structural grain. We have examined an area of approximately 600 km^2 in Danko area (Fig. 2) of Kebbi state, Nigeria. The resulting depth to magnetic basement map, that is, depth to the magnetic rocks that form the basement beneath the overlying non-magnetic rocks, sediments and soil, offers a guide for future mineral exploration projects.

2 Geologic setting and orogenic events

Our study area is around Danko area, which falls between latitudes 11°30′00″N and 11°45′00″N and longitudes 5°00′00″E and 5°15′00″E (Fig. 1), within the Proterozoic Zuru schist belt. The belt comprises of muscovite schists and quartzites, with minor quartz and pegmatite veins ([17], Fig. 2). The belt is probably the largest schist belt in NW Nigeria, with 280 km in length and with a width 40 km (Fig. 3). Structurally, the area is situated in a strained region, where rock units are affected by two

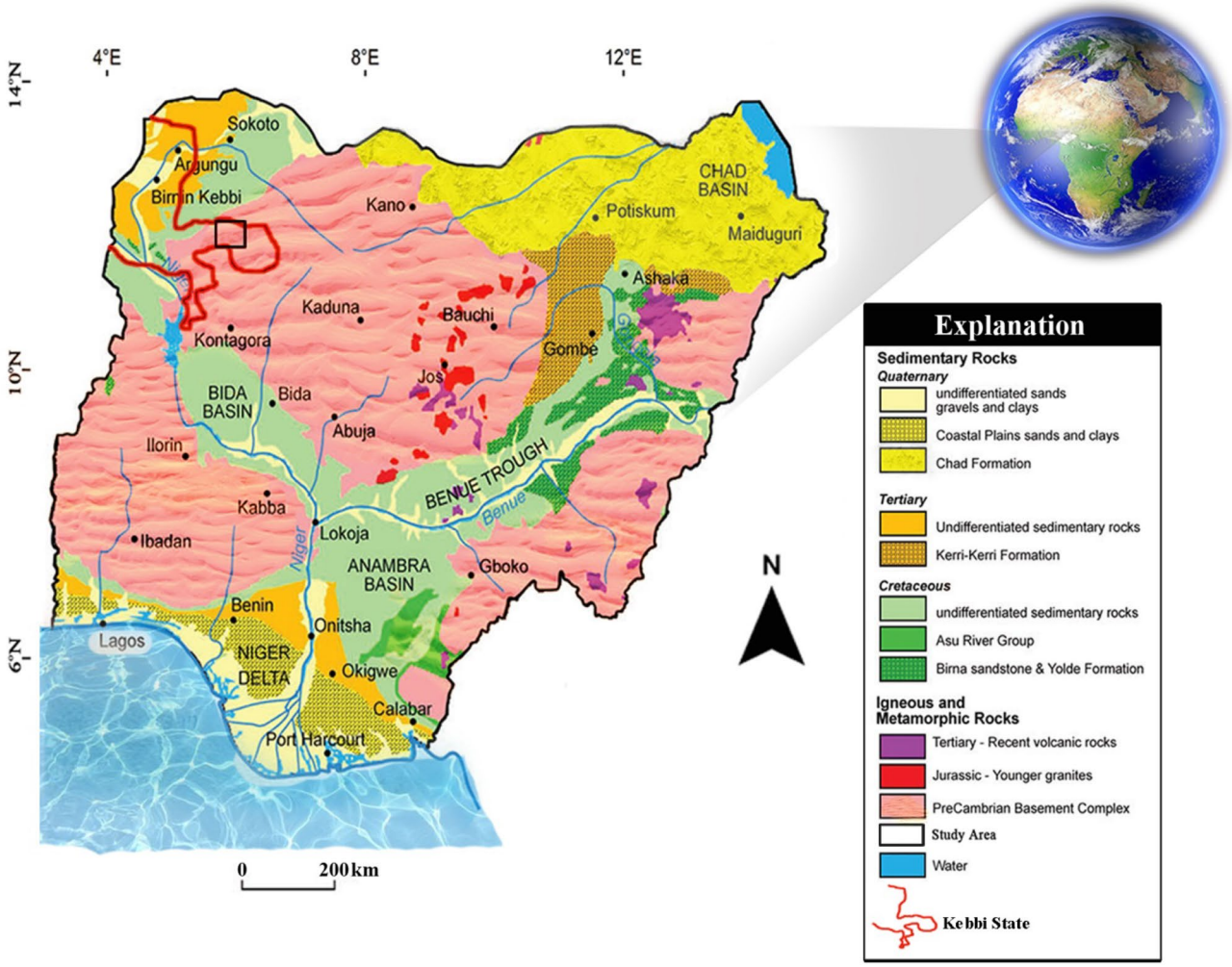

Fig. 1 Simplified geologic map of Nigeria showing the study area (modified after MacDonald et al. [38])

deformation episodes [18] and the deformational pattern exposed within the area is rather complex with variable geologic structures [19]. Younger Neoproterozoic N-trending geologic structures (Pan-African) are superimposed on beddings relative to older Palaeo- to Mid-Proterozoic (Eburnean) folds with E trends. A marked discontinuity separates the Zuru Schist to the south from the Anka belt with its steep geologic structures, though the contacts of the belt demonstrate parallel trends.

The Anka schist belt comprises of both Kibaran and Pan-African elements. A probable Kibaran igneous feature is the metamorphosed complex of ultramafic and mafic rock units and widespread epidotized pegmatite and granite that spreads for 100 km laterally east side of the Anka schist belt [19]. The connection between the Zuru quartzites and the Anka pelites is yet to be documented [20], and the relationship of their perceived contemporaneity notwithstanding, it would appear that the Anka unconformably overlies the Zuru, with the former possibly postdating the latter.

The main tectonic feature of the study area is the NE-trending Yelwa fault. This important structure is part of the NNE-trending Anka–Yauri transcurrent fault associated with gold mineralization [21, 22]. The Yelwa fault cuts across the Zuru schist and separates units; it is a fault thought to be in age. Identifying the Yelwa fault and any associated geologic structures in the subsurface would help focus future mineral exploration, and aeromagnetic data are well suited to highlight such structures.

2.1 Orogenic events

The entire Nigerian basement carries the imprint of the heterogenous Neoproterozoic Pan-African deformation [23], resulting in the reworking of the older crust, of

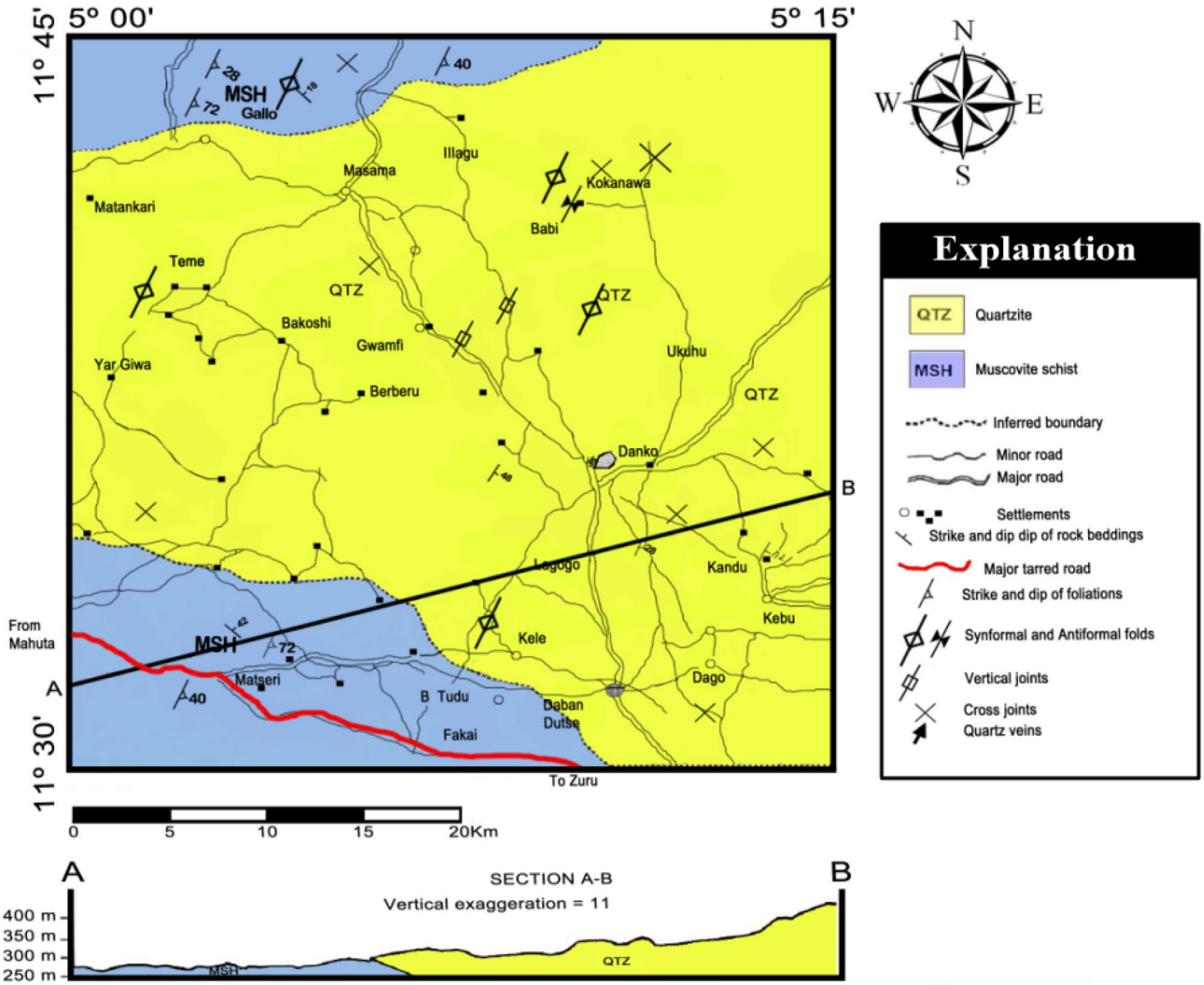

Fig. 2 Geologic map of the study area (modified after Umaru [15])

Liberian (2700 ± 200 Ma), Eburnean (2000 ± 200 Ma) and a probable Kibaran (1100 ± 200 Ma) [19, 24]. Structural and geochronological data by McCurry [18] provide evidence that the Eburnean and Pan-African orogenies are discernible within the study area.

The Eburnean tectonic events evidently affected a large region of Nigeria which was possibly accompanied by deformation, folding metamorphism, sedimentation and syntectonic igneous activity [18, 19, 24–27]. While the Paleoproterozoic Eburnean (2.2 Ga) event was essentially accretionary [27, 28], the Pan-African (600 Ma) was largely thermotectonic in nature, reworking preexisting terranes through widespread deformation, granitization, migmatization and intrusion of complete range of granitoid units at higher temperatures ($T \geq 600$°C) [22]. The tectonic events also imposed dominant N-trending structural features, on the region which define the structural fabrics of the entire Nigeria [19].

3 Method

The high-resolution aeromagnetic anomaly map (SW segment of sheet 74) provided by the Nigerian Geological Survey Agency (NGSA) in grid form was used for this study. The aeromagnetic anomaly data cover parts of Danko area, northwestern Nigeria (Fig. 4). The data were acquired as part of the national high-resolution airborne geophysical survey, flown over the entire country of Nigeria, which was carried out by Fugro Surveys, for the NGSA in the year 2003 to 2009. It was acquired using 3 × Scintrex CS3 cesium vapor magnetometer along a sequence of flight lines oriented in NW–SE, with line spacing of

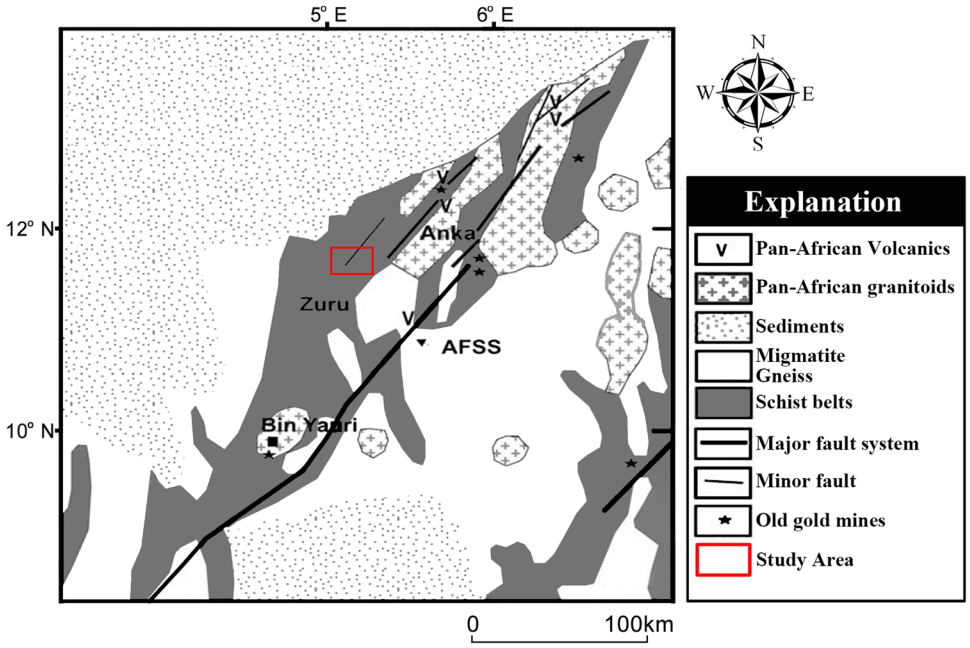

Fig. 3 Regional geologic map showing the Zuru and Anka schist belts with the major NNE–trending Anka–Yauri fault associated with gold mineralization (modified after Dada [22], Garba [39])

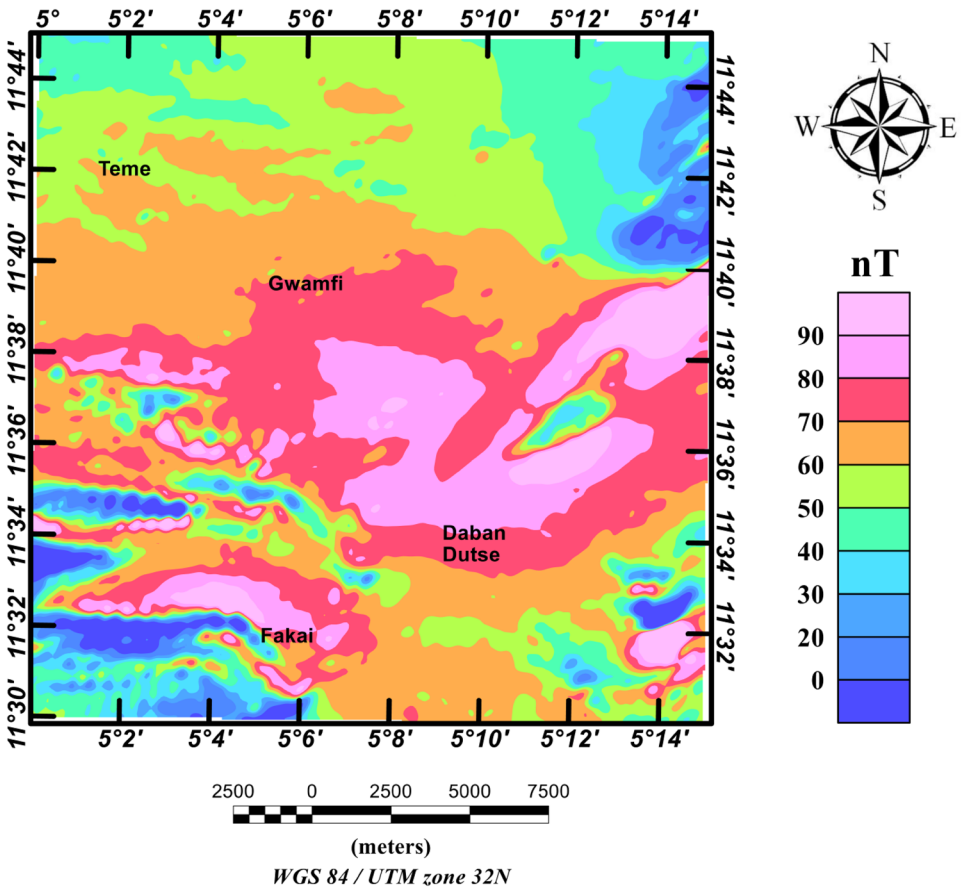

Fig. 4 Total magnetic intensity anomaly map of the study area

500 m, sensor mean terrain clearance of 80 m and tie lines of 2000-m interval. The data were corrected for diurnal variation effects and was gridded by one-dimensional interpolation, perpendicular to flight direction, since no significant, high-frequency anomalies occur at shallow depths that can cause aliasing in the total magnetic

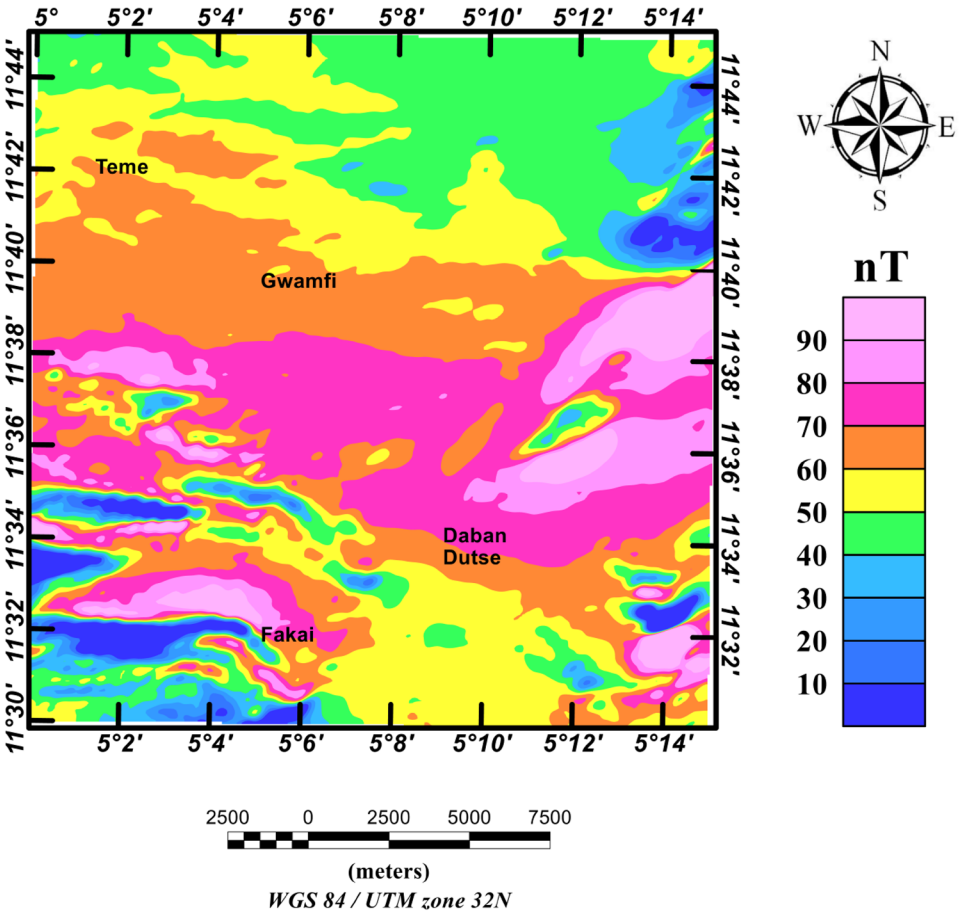

Fig. 5 RTE aeromagnetic anomaly map of Danko the study area

intensity (TMI) data. The TMI refers to the vector resultant of the strength of both geomagnetic and crustal fields. The International Geomagnetic Reference Field (IGRF) was applied to the aeromagnetic data by NGSA to remove the geomagnetic field effect. The IGRF and diurnal-corrected TMI anomaly map is shown in Fig. 4. The TMI anomaly map was enhanced in order to image subsurface geologic structures of the study area, by applying several standard derivative and match filtering techniques. All processing was performed using commercial software package Oasis Montaj (Geosoft™).

The results of the match filtering and derivative-based techniques can be quite uncertain, and it is therefore important to apply different filters, each of which leverages a slightly different aspect of the aeromagnetic anomaly data, and see whether the results are in agreement or whether they are contradictory. If the former was the case, then confidence grows that the results have some physical meaning in terms of the subsurface geology. Magnetic anomalies are shifted in map view from their source at nonpolar and non-equatorial latitudes; we first apply a filter that centers anomalies over their sources and also suitable for low-latitude regions. We chose the reduction-to-equator (RTE) filter, by assuming that the observed magnetic field is due to induced magnetic effects. The assumption of induced magnetization is based on the fact that no volcanic rocks exist in the region. Parameters for applying the reduction-to-equator filter are the inclination, declination and total magnetic intensity for the study area. We chose the values of these parameters at the midpoint of the Danko study area (longitude 5° 8′E and latitude 11° 38′N): inclination of 0.476 degrees, declination of − 1.875 degrees and total field value of 33,755 nT. After application of the filter, the anomalies of the resulting RTE anomaly map (Fig. 5) are shifted such that they are centered over their respective sources.

3.1 Regional–residual separation using matched filtering

Matched filtering is an effective approach of separating magnetic anomalies from various depths. The technique is based on fitting lines to the radially averaged power spectrum of the RTE aeromagnetic anomaly data, with a series of power spectra corresponding to equivalent layers (a magnetic anomaly has an equivalent surface distribution of magnetization at depth, known as equivalent layer) at different depths within the study region [29]. Each linear

segment of the power spectrum is interpreted as a subsurface geologic layer in which magnetic source bodies are present. For the Danko study area, the radially averaged power spectrum curve (6a) was divided into three linear segments, representing three separate geologic layers of magnetic sources. Once the layers have been defined, each component can be separated from the RTE map using a band-pass filter (a Butterworth filter is a convenient option) and then individually analyzed further. Butterworth filters have the advantage of straightforward application of low-pass and high-pass filters to the RTE anomaly data, since the degree of filter roll-off can easily be controlled, while the central wavenumber remains fixed. When ringing is detected, the degree is normally reduced to achieve an acceptable result. The depths to top of the subsurface layers (5b) are estimated based on the slope of the linear segments of the power spectrum curve (5a) using the following formula:

$$Z(\text{depth}) = \frac{-\text{slope}}{4\pi} \tag{1}$$

3.2 Edge detection methods

3.2.1 Horizontal gradient magnitude (HGM)

Edge detection methods are essential tools for delineating the edges, and hence the horizontal extent, of magnetic source bodies, and in Danko area, these could be where the Zuru schist was offset by faulting or changes lithology. The edges of magnetic sources within Danko area can be examined by applying the horizontal gradient magnitude. The horizontal derivatives (the horizontal gradient magnitude is the vector sum of the horizontal derivatives) of the magnetic field in a presume direction enhances lateral changes in the magnetic field while attenuating its regional trend along that direction. Normally, in the locations where magnetic susceptibility difference is highest, the derivative will attain a maximum; this highlights discontinuities perpendicular to the direction of derivation and indicates the edges of geologic structures [6, 7]. Identifying the maximum horizontal gradient is a straightforward technique for highlighting potential edges of subsurface magnetic source bodies. When horizontal gradient maxima are aligned linearly, it can be interpreted as a linear contrast in magnetic properties, i.e., the edge of a magnetic source body. This technique therefore involves finding places where the local maxima in the HGM are aligned, and magnetic source body edges can be interpreted at these locations. Note that the maxima are strongest when the edges are oriented vertically; edges that deviate from vertical too much do not produce local gradient maxima. The HGM technique requires calculating the two first-order horizontal derivatives of the magnetic field, which makes it insensitive to the noise in the magnetic data [9]. If $M(x, y)$ is the total magnetic intensity at location (x, y), the HGM is given as:

$$\text{HGM}(x, y) = \sqrt{\left(\frac{\partial M}{\partial x}\right)^2 + \left(\frac{\partial M}{\partial y}\right)^2} \tag{2}$$

where the horizontal derivatives are $\partial M/\partial x$ and $\partial M/\partial y$ of the aeromagnetic data. The HGM was calculated for the RTE grid data of the study area. Peaks of the HGM were extracted by passing a small 3 by 3 window over the grid and searching for peaks [30].

3.2.2 Tilt derivative (TDR) method

The aeromagnetic anomaly maps are utilized to specify regions of significant magnetic contrast and to depict structural features such as dykes and faults. The edge detection techniques are utilized for outlining structural features which can depict major fault and any associated geologic structures with Danko area. One of the standard techniques is TDR, an edge detection technique. The TDR technique is used for mapping shallow geologic structures in solid mineral exploration, because the method excels at detecting edges of magnetic source bodies. The technique was initially described by Miller and Singh [12] and was further developed by Verduzco et al. [13] and given as:

$$\text{TDR} = \tan^{-1}\left(\frac{\text{VDR}}{\text{HGM}}\right) \tag{3}$$

where the vertical derivative is given as VDR and total horizontal derivatives are given as HGM.

The amplitudes of tilt angle derivative range between −90° and +90° [−π/2 and +π/2 (radian)] irrespective of the amplitude of the VDR or the absolute value of HGM [13, 31]. The TDR differs markedly with inclination; however, for inclinations of 0° and 90° its zero crossing is situated very close to 2D magnetic source body edges such as blocks, steps and dikes [13]. Though reduced-to-equator and reduced-to-pole transformations work adequately for TDR filter, the RTE anomaly field is preferred since the study area is close to the magnetic equator [13]. It should be noted that for reduced-to-equator transformation, the amplitudes of the TDR are negative over magnetic source bodies, and are positive outside the magnetic source bodies.

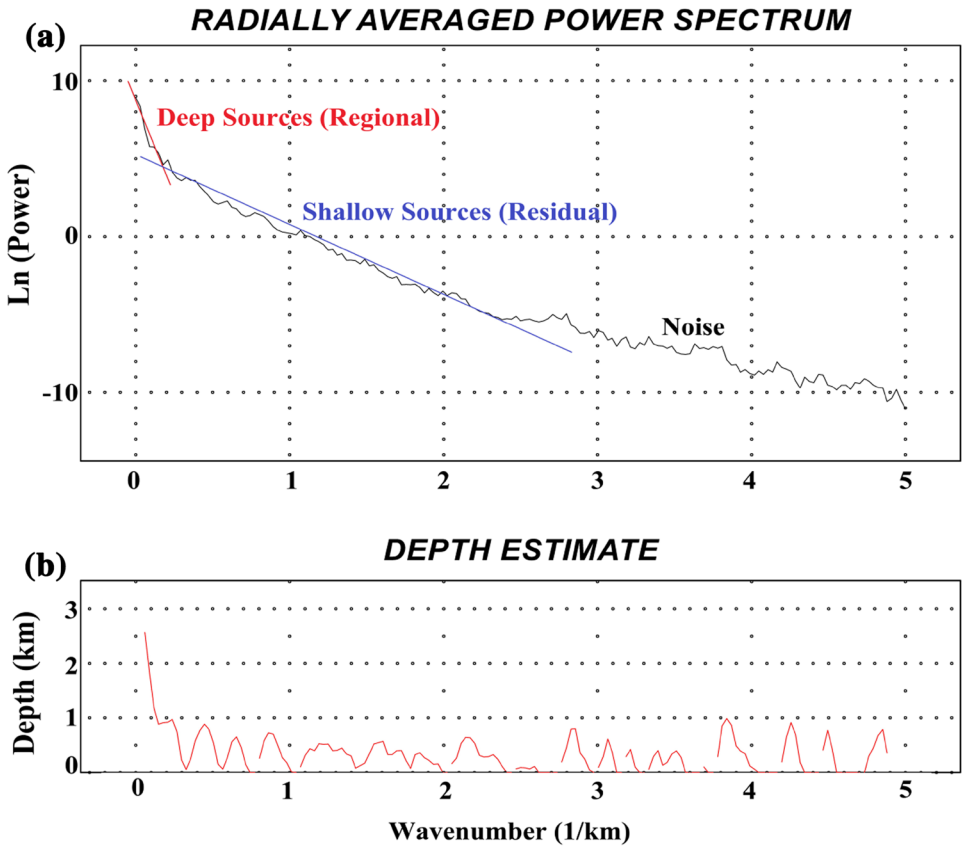

Fig. 6 **a** Averaged power spectrum plot of the RTE aeromagnetic anomaly data of Danko area, **b** depth estimates for magnetic source bodies based on linear segments of the power spectrum curve

3.3 Depth to basement estimation

3.3.1 Analytic signal (AS) method

The analytic signal (AS) method has been successfully utilized to provide reliable descriptions of 2D magnetic source body parameters such as detection of edges and depth estimates [7, 11]. In particular, this filter is able to estimate depths to various magnetic source bodies, and in Danko area, these could be related to mineral exploration targets. The AS depth map presents various forms of results depending on the characteristic of the source geometry called structural index (SI) [32] and the choice of SI. The SI is a measure of the rate of decay of the magnetic field $M(x, y, z)$ with distance from the magnetic source body at (x_0, y_0, z_0) [8]. The main advantage of the AS method, initially established for profile magnetic data by Nabighian [10], is its lack of dependence on magnetization direction (inclination), when estimating magnetic parameters from 2D magnetic source bodies [11, 33]. This is a major advantage over previous mentioned techniques (TDR and HGM) since their algorithm usually requires that the aeromagnetic anomaly data undergo either a reduction-to-pole or reduction-to-equator transformation. The AS filter is less sensitive to the interference effects between nearby anomalies and noise in the magnetic data [7, 11]. The peaks of the AS amplitude, which are deduced from the vertical and first horizontal derivatives of the observed magnetic field, are normally use to locate the edges of magnetic source bodies and estimate their strike directions [11, 13].

The AS filter is given as:

$$AS = \sqrt{\left(\frac{\partial f}{\partial x}\right)^2 + \left(\frac{\partial f}{\partial y}\right)^2 + \left(\frac{\partial f}{\partial z}\right)^2} \tag{4}$$

where the first derivatives $\frac{\partial f}{\partial x}$, $\frac{\partial f}{\partial y}$, $\frac{\partial f}{\partial z}$ of the total magnetic field are in the x, y and z directions.

The AS is highly important interpretative technique, because the depths and locations of magnetic anomalies are estimated with little assumptions with regard to the nature of the anomalies, which is normally presumed to be 2D magnetic source bodies (e.g., dike, contact and step) [9]. The depths of magnetic anomalies are estimated using the following relation [4]:

$$AS1 = \sqrt{\left(\frac{\partial fv}{\partial x}\right)^2 + \left(\frac{\partial fv}{\partial y}\right)^2 + \left(\frac{\partial fv}{\partial z}\right)^2} \tag{5}$$

On the maximum amplitude,

$$D = \frac{AS}{AS1} * N \tag{6}$$

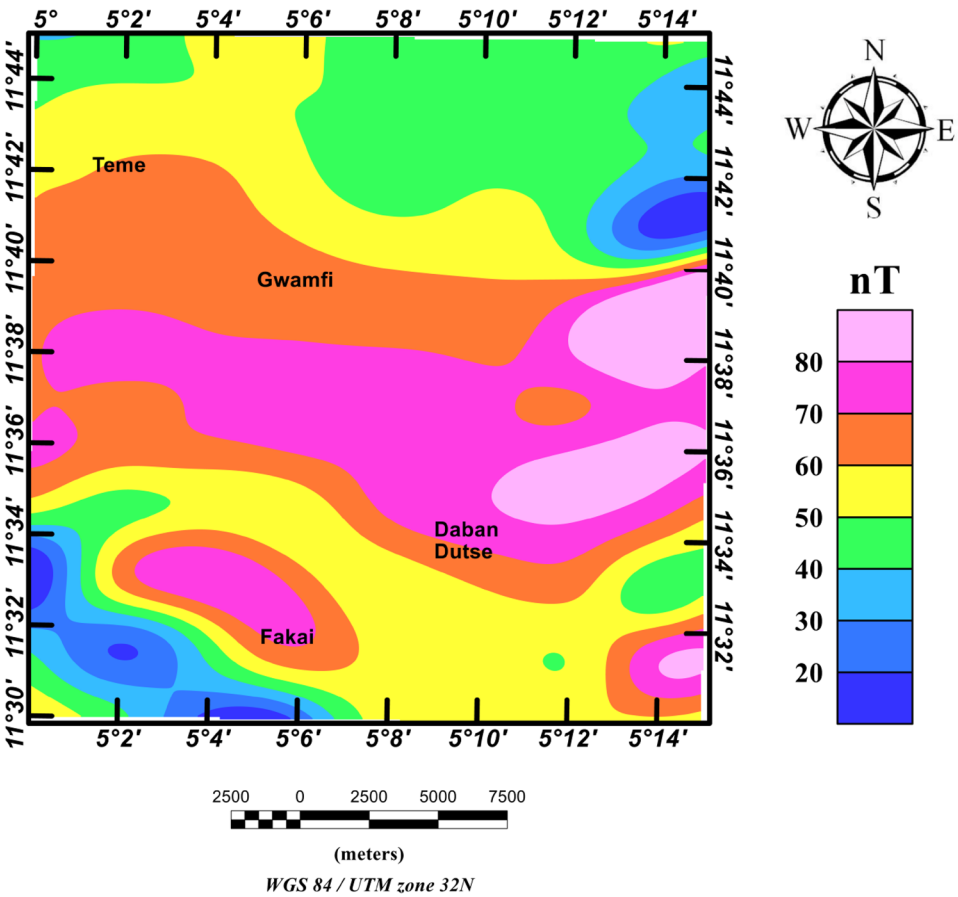

Fig. 7 RTE regional magnetic anomaly map of Danko area

where the first vertical derivative of the RTE magnetic field is given as *fv*, depth to the magnetic sources is given as *D*, analytic signal of the RTE aeromagnetic map is given as *AS* and analytic signal of first vertical derivative of the RTE aeromagnetic map is given as *AS*1. The structural index (*N*) is related to the geometry of the magnetic anomalies, e.g., $N=1$ (contact), $N=2$ (dike), $N=3$ (pipe) and $N=4$ (sphere) [32].

4 Results and discussion

The total magnetic intensity (TMI) aeromagnetic anomaly map of the study area (Fig. 4) depicts magnetic anomaly values between 0.0 to 90 nT. Since the area under study is much closer to the magnetic equator, magnetic source bodies tend to be characterized usually by low negative anomalies instead of high positive anomalies. The TMI map shows prominent low-amplitude anomalies in both elongated and circular shapes distributed at the northeastern and southwestern parts of the map with NE and E trends.

The reduction in the magnetic equator (RTE) map (Fig. 5) shows positive and negative magnetic sources of various wavelengths and amplitudes with values, which range from 10 and 90 nT. Also, The RTE filter has centered these magnetic anomalies over their respective sources, so the resulting map is easier to interpret. Visual analysis of the RTE map indicates that the map can be divided in two major domains, according to the amplitudes and trends of the anomalies.

1. The first domain at the southern and northern part of the study area is characterized by medium to low anomalies along the western edge of the study area, extending from Teme south to Fakai. These anomalies are interpreted as muscovite schist units. The E-trending structural grains within the domain reflect an early ductile deformational phase (D1), which are probably Eburnean (pre-Pan-African) in age.
2. The second domain in the central part of the study area emphasizes high positive anomalies which extend from Gwamfi to Daban Dutse and Fakai areas. The anomalies are interpreted as quartzite units and are suspected to have been emplaced on the muscovite schist belt during the thrust fault event, shown by the later NE ductile–brittle deformation (D2) phase [17] attributed to late Pan-African event at the eastern part the study area.

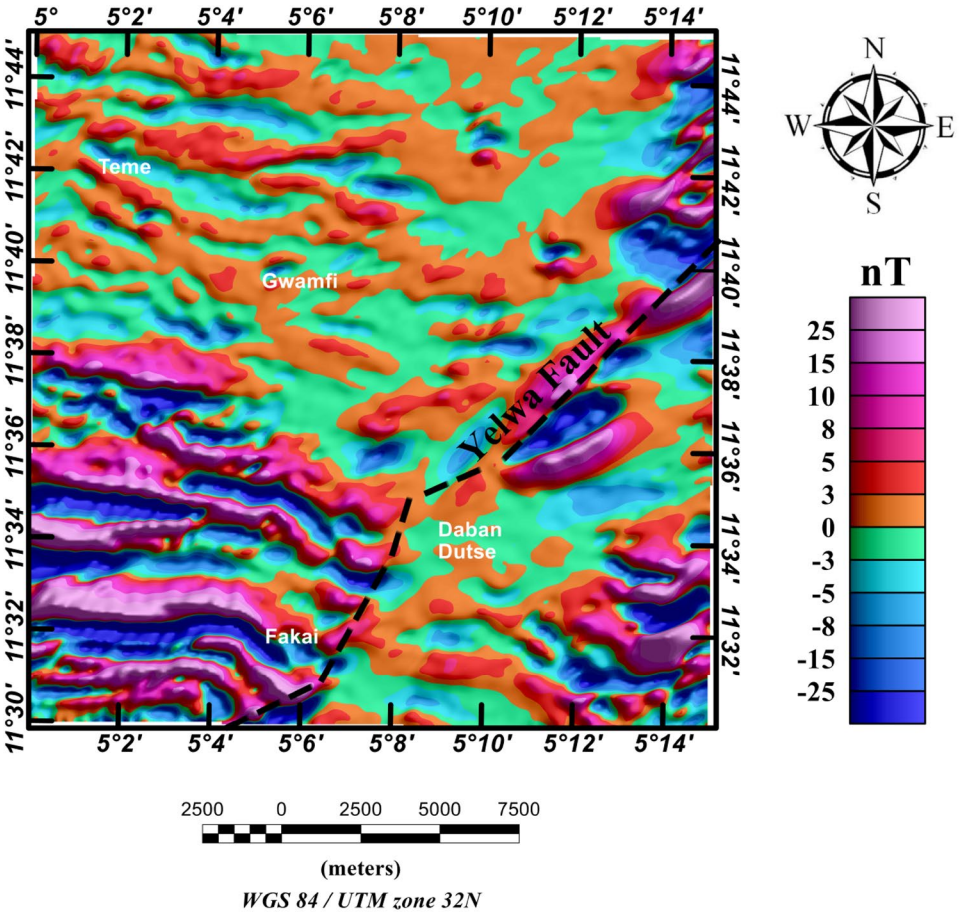

Fig. 8 Color-shaded RTE residual magnetic anomaly map of Danko area

In order to further investigate the subsurface geologic structures, we applied the matched filtering technique to the RTE anomaly data to determine estimates of depth for the major source bodies in the study area. The average power spectrum curve for the RTE aeromagnetic anomaly map of Danko area is shown in Fig. 6; this curve was used to determine the regional and residual sources and to define the noise component. Also, the resulting depth estimate chart was used to estimate the average depths to the top of the shallow and deep anomalies. The estimated depth to the top of shallow sources is 500 m, while the deeper sources are 1000 m (Fig. 6). The linear segments, approximating the curve in Fig. 6a, are used to define the cutoff wavelength between the shallow and regional magnetic sources, and this corresponds to a depth of 500 and 1000 m for the top of the shallow and regional sources, respectively.

The regional (low-pass) magnetic anomaly map (Fig. 7) allows us to accurately divide the deeper magnetic lithological units into three major lithological domains. The subdivision into lithological domains is coherent with the visual analysis of the regional anomaly map. In the central portion of the regional anomaly map allows the identification of a lithological domain, with strong E-trending positive magnetic anomalies, interpreted to be associated quartzite units. The northern and southern parts of the regional anomaly map reflect similar patterns with low magnetic anomalies interpreted to be associated with muscovite schist units.

The high-pass (residual) magnetic anomaly component map (Fig. 8) shows high- (magenta to yellow color) and low-/negative (green and blue colors) amplitude anomalies corresponding to shallow-seated magnetic geologic sources. These shallow magnetic source bodies have mainly E and NE trends, are widely distributed across the map with elongated shapes and are characterized by their alternating high frequencies and low magnetic anomalies. These variations are interpreted as the upper basement composed of crystalline rocks containing relatively high magnetite content. In the eastern portion of the residual anomaly map, many of the E-trending anomalies are truncated, and these truncations form a major NE elongated lineament. The lineament exhibits a good geometric correlation with the documented Yelwa fault of McCurry [18], shown in Fig. 3. In the western portion of the map, the most prominent features are the high- and low-amplitude E-trending magnetic anomalies, which we interpret as

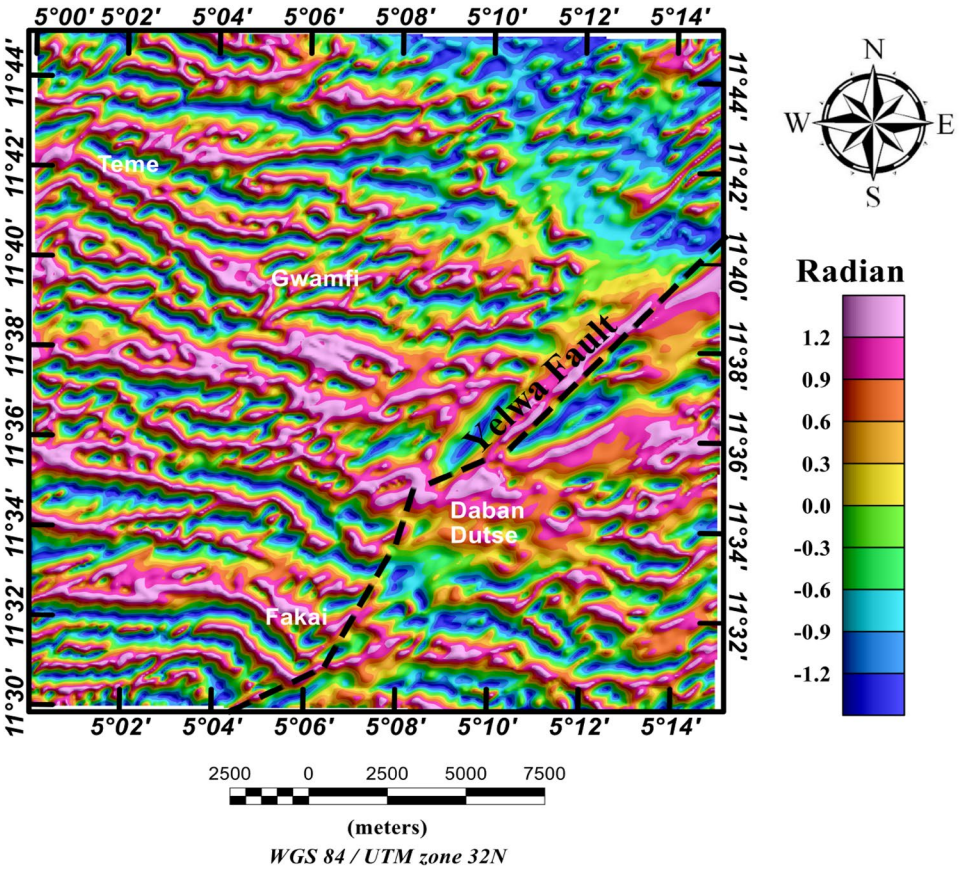

Fig. 9 Color-shaded TDR map of RTE aeromagnetic anomaly data of Danko area

changes in magnetic texture in the underlying muscovite schist and quartzite rock units located in Fakai and Gwamfi to Teme. The alternating nature of the E-trending anomalies likely indicates folding and faulting in the underlying muscovite schist and quartzite rock units. The northwestern E-trending anomalies reveal early D1 phase which is truncated about halfway across the study area by a later D2 phase, and the structural grain changes from E to NE trends.

The TDR filter is normally utilized in the detection and mapping of geologic structures which can be related to shallow basement structural features or mineral exploration targets. The TDR filter was applied to the RTE anomaly data, to provide greater resolution of structural features. The TDR map (Fig. 9) demarcates possible edges of geologic source bodies. The TDR technique facilitates the horizontal location with the extent of edges of magnetic source bodies within the study area. When utilizing the RTE transformation, the TDR is negative (blue and green color) when it is over magnetic source bodies and is positive (orange and magenta colors) when it is outside the magnetic source bodies. The zero contours on the TDR map are the positions of sharp transitions in magnetic susceptibilities between negative and positive magnetic source bodies. Consequently, the contact boundary or edges of magnetic source bodies are represented by the zero contours on the TDR map (also indicated by the transition from green to yellow color). The magnetic source bodies demarcated on the TDR map show the same overall pattern as seen in the residual match filter map—on the western side of the study area magnetic source bodies are linear and trend east, in the northeast the source bodes are more massive, and the Yelwa fault can be seen as a significant discontinuity cutting across the map. The TDR map of the region suggests that the rocks of Danko area have been affected by possibly two very close cycles of deformations. These are the early D1 episode attributed to Eburnean event and late D2 episode ascribed to Pan-African event.

The horizontal gradient magnitude (HGM) was applied on the RTE aeromagnetic anomaly data of Danko, as another alternative for detecting the edges of magnetic structures; the resulting map is shown in Fig. 10. Long, linear crests of the horizontal gradient magnitude of the RTE magnetic anomaly data demarcate the edges of magnetic source bodies. The linear crests can be quantitatively outlined, as described in the methods section. The resulting peaks of the HGM are plotted, along with the zero contour

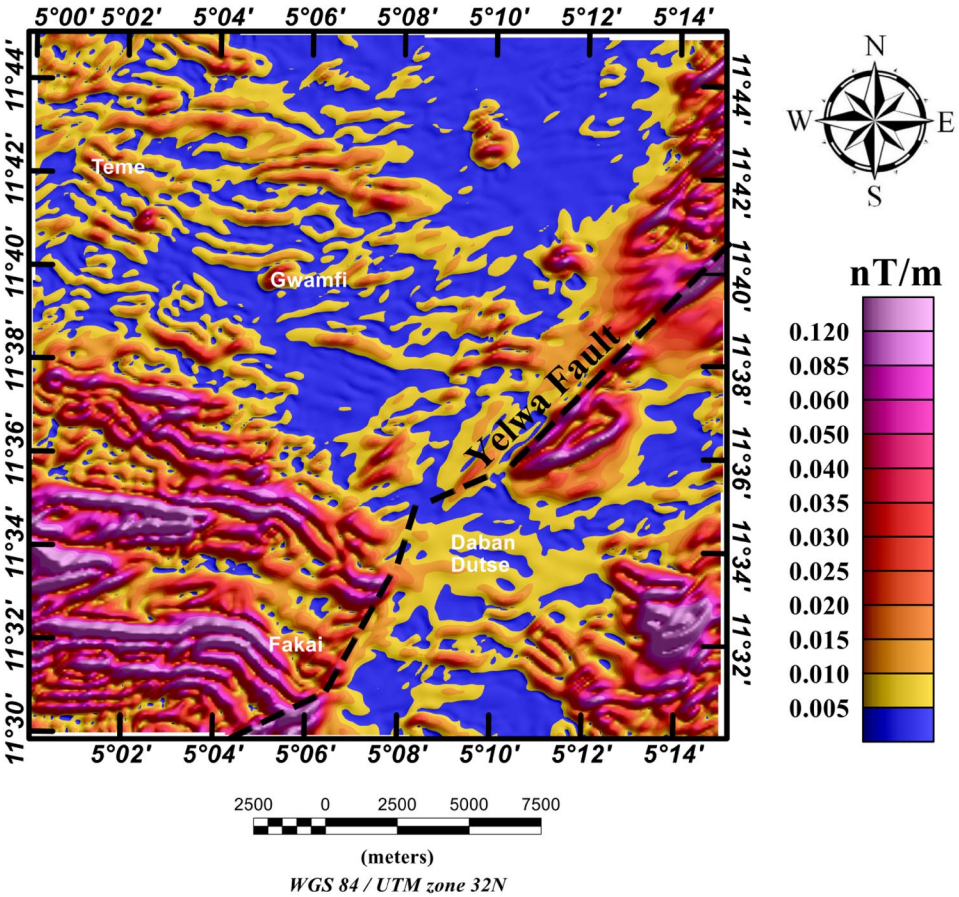

Fig. 10 Color-shaded horizontal gradient magnitude map of RTE aeromagnetic anomaly data of Danko area

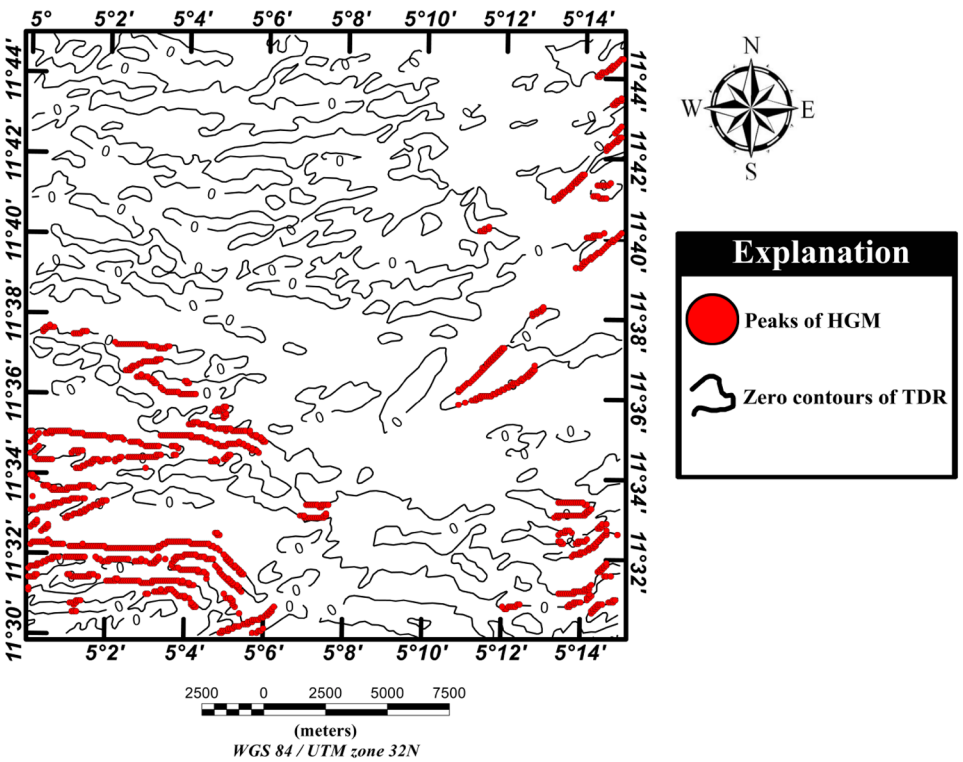

Fig. 11 Peaks of HGM plotted on TDR map of the Danko. The peaks are located on zero contour lines of TDR map

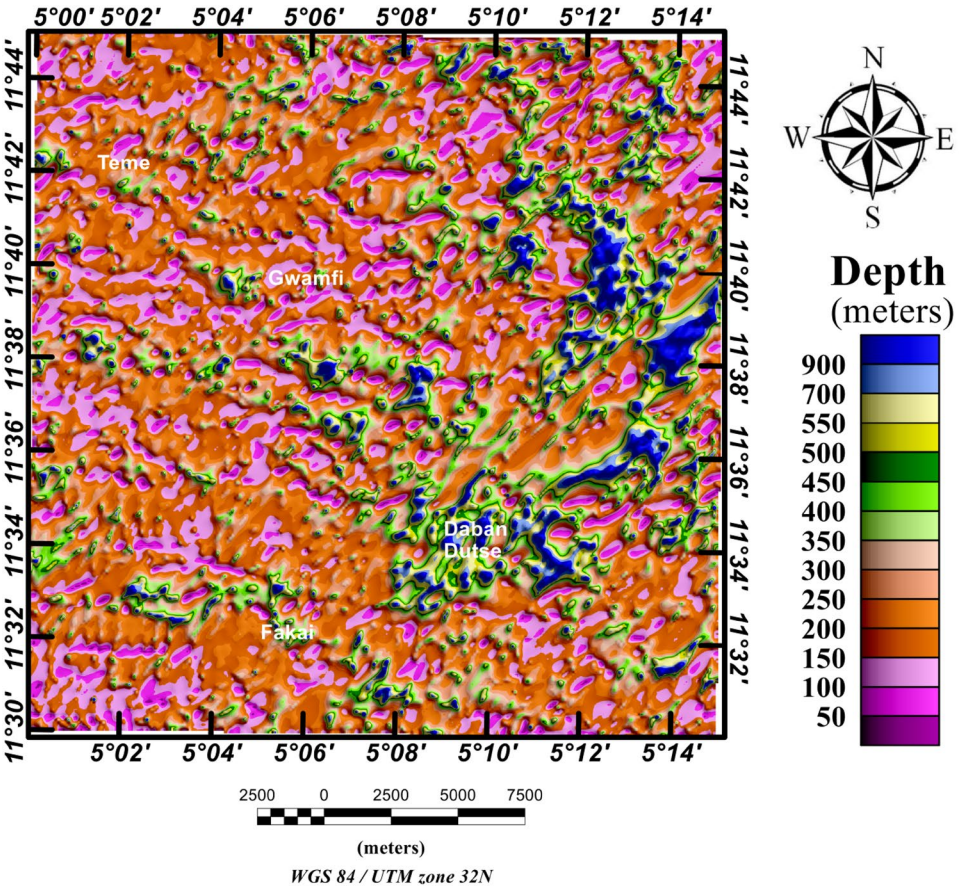

Fig. 12 Color-shaded depth to magnetic basement map deduced using the analytic signal method

lines of TDR, on the composite map in Fig. 11. A very good correlation can be seen between the peaks of the HGM and the zero contour lines of the TDR for the major features in the anomaly maps. The composite map (Fig. 11) reveals structural complexity within the region under study. Two major structural domains were recognized from the composite map, by changes in inferred lineament patterns, such as spacing and orientation.

1. The southwestern domain which was affected by a major ductile deformation (D1) event resulted in E–W trends of what we interpret as faults and folds in the muscovite schist and quartzite rock units, which are probably Eburnean (pre-Pan-African) in age.
2. The eastern domain which was affected by a major ductile–brittle deformation (D2) event which resulted in major NE–SW trends in the quartzite rock units. The tectonic activities with the Pan-African compression with the dominant temperature situations could have led to D2 deformations.

The analytic signal (AS) technique was implemented to deduce the magnetic basement configuration of the study area, which underlies the regolith and serves as the main impediment to exploration projects with the study area. From Eq. (6), the analytic signal of the RTE aeromagnetic map was divided by the analytic signal of first vertical derivative RTE aeromagnetic map (*AS*1) to properly produce the magnetic basement depth map of the study area (Fig. 12). The resulting depth map shows spatial location of different magnetic source bodies at various depths, thus providing more details than the match filtering. In general, the depth ranges between 50 m and 900 m. The frequency of the depth values shown in the magnetic depth map appears rather high; that is, spatially it appears to be a rather short distance between low and high depth values. This is interpreted as the depths to magnetic property distribution within the muscovite schist and quartzite units, such as quartz veins, pegmatite intrusions and intense folding of the schist into the into the migmatite–gneiss–quartzite complex. The average depth value of the magnetic basement depth map is 475 m, indicating a compelling alignment of result with the 500 m depth for the residual matched filter layer deduced from the average power spectrum plot (Fig. 6).

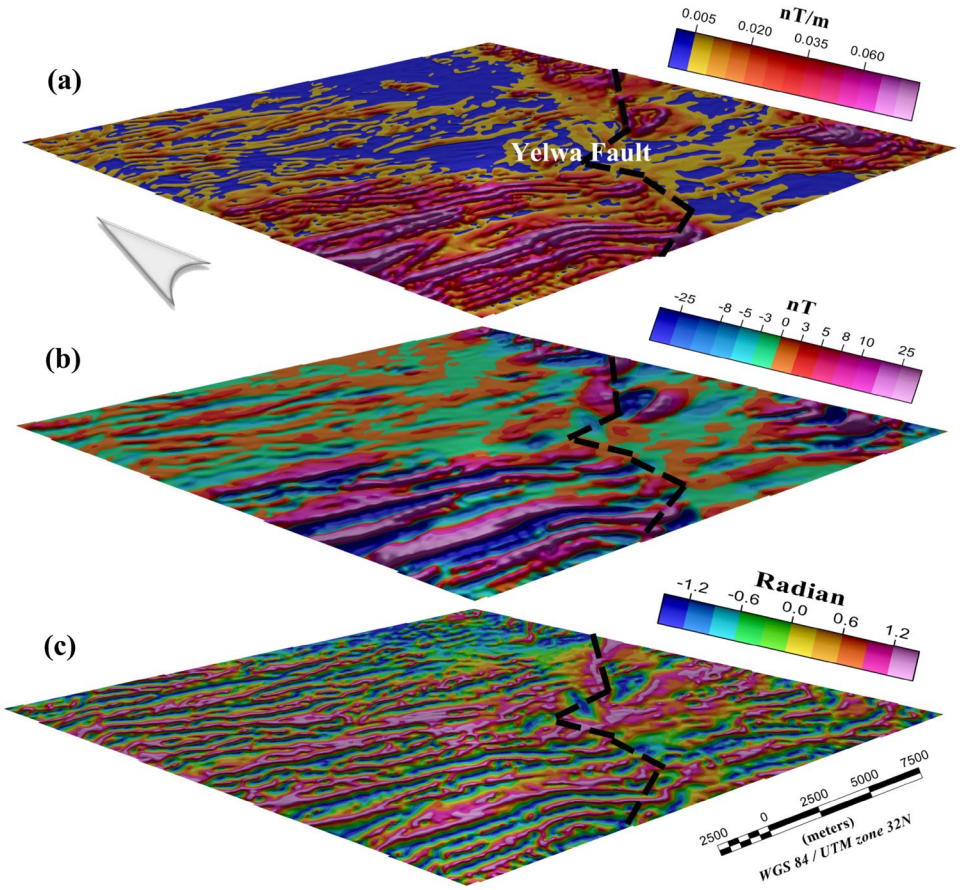

Fig. 13 Comparison of the color-shaded derivative maps of the study area: **a** horizontal gradient magnitude map; **b** residual magnetic anomaly map; **c** tilt derivative map. Note the complete extent of the Yelwa fault on the derivative maps indicated as dashed black lines

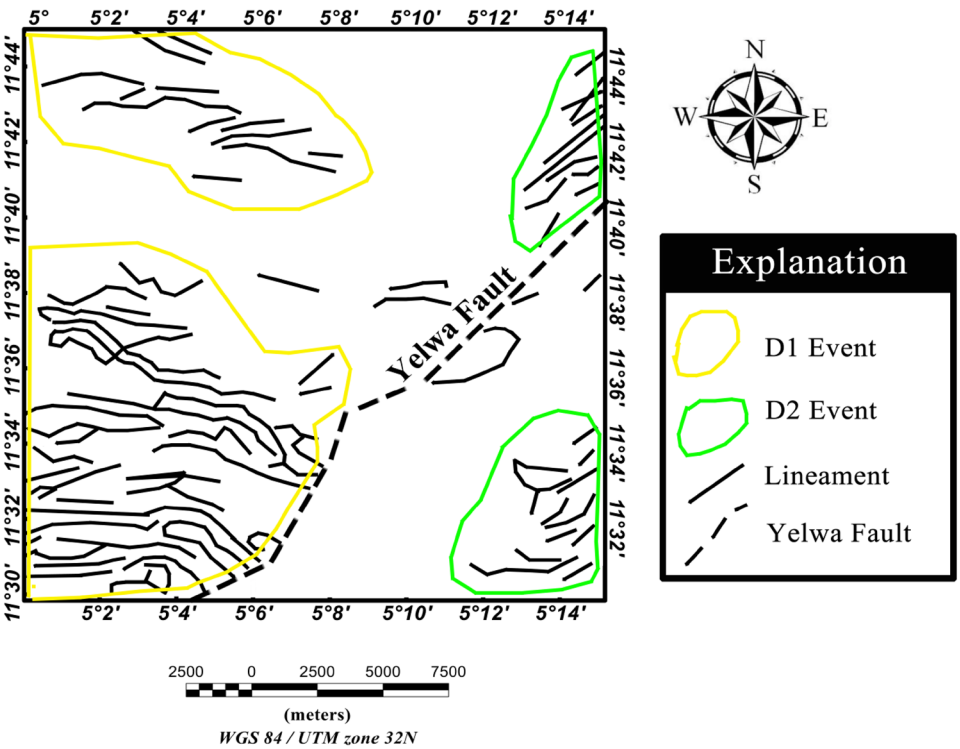

Fig. 14 Structural map of Danko area with detailed structural interpretation of the derivative maps, D1 event (enclosed in yellow polygons) attributed to Eburnean orogeny, D2 event (enclosed in green polygons) ascribed to Pan-African orogeny

4.1 Mineralization

The Pan-African restructuring and concentration of mineral deposits can be discussed in relation to structural controls and rock associations. For instance, the three main NNE–SSW-trending Yelwa, Zuru and Ribah wrench faults (Fig. 3) have been extensively acknowledged as probable Pan-African crustal sutures [34–36] and as locus of economic mineral deposits [22]. Numerous mineral exploration programs have been carried out in schist belts within surrounding regions of the study area (Yauri, Dogon Daji and Garin Hawal, e.g., Ramadan and Abdel-Fattah [37]). Many of these areas host gold, pyrite and Fe–Mn mineralization. The gold-bearing veins, stingers and reefs are mostly localized by ductile and brittle fault structures or planes of schistosity that traverse schists, phyllites, gneisses, quartzites and contact aureoles of granitoid masses. In the past and due to the trial-and-error techniques, these regions have experienced extreme artisanal mining which targets primary gold–quartz reefs [37]. This caused damages in many nonproductive locations, with obvious loss of land for agricultural production. Any significant mineral discovery will therefore be at depth hitherto unreached by artisanal miners. This makes geophysical methods such as aeromagnetic and a combination of ground magnetics and electrical methods more appropriate than geochemistry that would give spurious results in such brown fields. Hence, the results from this study present promising locations for structurally controlled mineralization. The complete extent of Yelwa fault is indicated on all the deduced derivative maps as shown in Fig. 13. Visual analysis of the derivative maps leads to the production of a structural map (Fig. 14) of the study area. The summary of outcomes achieved from the structural investigation of Danko area is shown in the structural map in Fig. 14.

5 Conclusion

An aeromagnetic dataset was used to analyze the subsurface geology of the Danko region of Kebbi State, to highlight magnetic source bodies forming the geologic structure of the region. Using standard techniques, several aspects of the subsurface were identified. The location of edges of the magnetic source bodies and estimation of magnetic basement depths from aeromagnetic anomaly map of Danko area of Kebbi State provide an indirect insight into subsurface architecture.

The results of HGM and TDR techniques in addition to the residual anomaly map help identify a prominent NE-trending fault suspected to be the documented Yelwa fault. Additionally, the results depict linear E-trending source bodies that we interpret as folding and faulting in the underlying quartzite and schist magnetic basement. The pattern of folding and faulting indicate two close cycles of deformation events. The western part of the study area was affected by the Eburnean, a major ductile deformation event that imprinted E-trending geologic structures. The eastern part was equally affected by another phase of ductile–brittle deformation, the Pan-African, which imprinted NE-trending geologic features in the region. The magnetic basement depth map deduced from the analytic signal method depicts high-frequency depth values which represent the magnetic property distribution within the muscovite schist and quartzite units: quartz veins, pegmatite intrusions and intense folding of the schist into the migmatite–gneiss–quartzite complex. The present study offers insights into structural framework of Danko area and can form basis for future mineral exploration studies within the region.

Acknowledgements The authors thankfully acknowledge the support of BS Geophysical and Consultancy Ltd., for their immense contribution and the facilities made available during the course of this research. We would like to thank the two reviewers for suggestions and comments that help improve the manuscript.

Compliance with ethical standards

Conflict of interest The authors declare that they have no conflict of interest.

References

1. Nabighian MN, Grauch VJS, Hansen RO, LaFehr TR, Li Y, Peirce JW, Phillips JD, Ruder ME (2005) The historical development of the magnetic method in exploration. Geophysics 70:33–61
2. Tsokas GN, Papazachos CB (1992) Two-dimensional inversion filters in magnetic prospecting: application to the exploration for buried antiquities. Geophysics 57:1004–1013
3. Salawu NB, Olatunji S, Orosun MM, Abdulraheem TY (2019) Geophysical inversion of geologic structures of Oyo Metropolis, Southwestern Nigeria from airborne magnetic data. Geomech Geophys Geo-energy Geo-Resour 5:143–157
4. Saada AS (2016) Edge detection and depth estimation of Galala El Bahariya Plateau, Eastern Desert-Egypt, from aeromagnetic data. Geomech Geophys Geo-energy Geo-resour 2:25–41
5. Salem A, Williams S, Fairhead D, Smith R, Ravat D (2008) Interpretation of magnetic data using tilt-angle derivatives. Geophysics 73:L1–L10
6. Cordell L, Grauch VJS (1985) Mapping basement magnetization zones from aeromagnetic data in the San Juan basin, New Mexico. In: Hinze WJ (ed) The utility of regional gravity and magnetic anomaly maps. Society of Exploration Geophysicists, pp 181–197
7. Roest WR, Pilkington M (1993) Identifying remanent magnetization effects in magnetic data. Geophysics 58:653–659. https://doi.org/10.1190/1.1443449
8. Phillips JD, Hansen OR, Blakely RJ (2007) The use of curvature in potential-field interpretation. Explor Geophys 38:111–119

9. Phillips JD (2000) Locating magnetic contacts: a comparison of the horizontal gradient, analytic signal, and local wavenumber methods. In: SEG technical program expanded abstracts 2000, pp 402–405
10. Nabighian MN (1972) The analytic signal of two-dimensional magnetic bodies with polygonal cross-section: its properties and use for automated anomaly interpretation. Geophysics 37:507–517. https://doi.org/10.1190/1.1440276
11. Roest WR, Verhoef V, Pilkington M (1992) Magnetic interpretation using the 3-D analytic signal. Geophysics 57:116–125
12. Miller HG, Singh V (1994) Potential field tilt: a new concept for location of potential field sources. J Appl Geophys 32:213–217
13. Verduzco B, Fairhead JD, Green CM, MacKenzie C (2004) New insights into magnetic derivatives for structural mapping. Lead Edge 23:116–119
14. Muzaffer ÖA, Ünal D (2013) Edge detection of magnetic sources using enhanced total horizontal derivative of the tilt angle. Yerbilimleri 34(1):73–82
15. Umaru AO (2016) Geology and structural evolution of Danko, sheet 74sw part of Zuru schist belt, northwestern Nigeria. Dissertation, Ahmadu Bello University, Nigeria
16. Binta H, Yaro SA, Thomas DG, Dodo MR (2016) Beneficiation of low grade manganese ore from Wasagu, Kebbi State, Nigeria. J Raw Mater Res 10(2):63–73
17. McCurry P (1976) The geology of the Precambrian to lower palaeozoic rocks of Northern Nigeria: a review. In: Kogbe CA (ed) Geology of Nigeria. Elizabethan Publishers, Lagos, pp 15–39
18. McCurry P (1978) Geology of degree sheets 19 (Zuru), 20 (Chafe), and part of 19 (Katsina). Overseas Geological Mineral Resource, Nigeria, p 53
19. Turner DC (1983) Upper proterozoic schist belts in the Nigerian sector of the Pan-African Province of West Africa. Precambrian Res 21:55–79
20. Obaje NG (2009) Geology and mineral resources of Nigeria, Lecture note in Earth science series, vol 120
21. Garba I (2000) Gold prospect of the Nigerian Pan-African terrain of West Africa. J Min Geol 36:123–156
22. Dada SS (2008) Proterozoic evolution of the Nigeria–Boborema province. In: Pankhurst RJ, Trouw RAJ, de Brito Neves BB, de Wit MJ (eds) West Gondwana: pre-cenozoic correlations across the south Atlantic region. Geological Society, London, Special Publications 294: 121–136. https://doi.org/10.1144/sp294.7
23. Annor AE, Freeth SJ (1985) Thermo-tectonic evolution of the Basement Complex around Okene, Nigeria, with special reference to deformation mechanism. Precambrian Res 28:73–77
24. Ajibade AC, Woakes M, Rahaman MA (1987) Proterozoic crustal development in the Pan African regime of Nigeria. In: Kröner A (ed) Proterozoic crustal evolution. American Geophysical Union, Geodynamic Series vol 17, pp 259–271
25. Grant NK (1970) Geochronology of Precambrian basement rocks from Ibadan, southwestern Nigeria. Earth Planet Sci Lett 10:29–38
26. Caen-Vachette M (1979) Orthogneiss birrimiens et migmatisation panafricaine au Togo-Bénin. R ~ surn ~ s 10 Colloque G ~ ol. Africaine, Montpellier, p 22
27. Annor AE (1995) U-Pb zircon age for Kabba–Okene granodiorite gneiss: implication for Nigeria's basement chronology. Afr Geosci Rev 2:101–105
28. Annor AE (1998) Structural and chronological relationship between the low grade Igarra schist and its adjoining Okene migmatite-gneiss terrain in the Precambrian exposure of southwestern Nigeria. J Min Geol 34:187–196
29. Sheriff SD (2010) Matched filter separation of magnetic anomalies caused by scattered surface debris at archaeological sites. Near Surf Geophys 8:145–150
30. Blakely RJ, Simpson RW (1986) Approximating edges of source bodies from magnetic or gravity anomalies. Geophysics 51(7):1494–1498
31. Salem A, Williams S, Fairhead J, Ravat D, Smith R (2007) Tilt depth method: a simple depth estimation method using first-order magnetic derivatives. Lead Edge 26:1502–1505
32. Reid AB, Allsop JM, Granser H, Millett AJ, Somerton IW (1990) Magnetic interpretation in three dimensions using Euler deconvolution. Geophysics 55:80–91
33. Pilkington M, Keating P (2006) The relationship between local wavenumber and analytic signal in magnetic interpretation. Geophysics 71(1):L1–L3
34. Wright JS (1976) Fracture systems in Nigeria and initiation of fracture zones in the South Atlantic. Tectonophysics 34:43–47
35. Mccurry P, Wright JB (1977) Geochemistry of calc-alkaline volcanics in Northwestern Nigeria, and a possible Pan-African suture zone. Earth Planet Sci Lett 37:90–96
36. Ajibade AC, Wright JB (1988) Structural relationships in the schist belts of Northwestern Nigeria. In: Oluyide PO et al (eds) Precambrian Geology of Nigeria. Geological Survey of Nigeria Publication, Kaduna, pp 103–109
37. Ramadan TM, Abdel Fattah MF (2010) Characterization of gold mineralization in Garin Hawal area, Kebbi State, Northwestern Nigeria, using remote sensing. Egypt J Remote Sens Space Sci 13:153–163
38. MacDonald AM, Cobbing J, Davies J (2005) Developing groundwater for rural water supply in Nigeria. British Geological Survey Commissioned Report CR/05/219N
39. Garba I (2000) Gold prospect of the Nigerian Pan-African terrain of West Africa. J Min Geol 36:123–156

Terms and Conditions

Springer Nature journal content, brought to you courtesy of Springer Nature Customer Service Center GmbH (“Springer Nature”).
Springer Nature supports a reasonable amount of sharing of research papers by authors, subscribers and authorised users (“Users”), for small-scale personal, non-commercial use provided that all copyright, trade and service marks and other proprietary notices are maintained. By accessing, sharing, receiving or otherwise using the Springer Nature journal content you agree to these terms of use (“Terms”). For these purposes, Springer Nature considers academic use (by researchers and students) to be non-commercial.
These Terms are supplementary and will apply in addition to any applicable website terms and conditions, a relevant site licence or a personal subscription. These Terms will prevail over any conflict or ambiguity with regards to the relevant terms, a site licence or a personal subscription (to the extent of the conflict or ambiguity only). For Creative Commons-licensed articles, the terms of the Creative Commons license used will apply.
We collect and use personal data to provide access to the Springer Nature journal content. We may also use these personal data internally within ResearchGate and Springer Nature and as agreed share it, in an anonymised way, for purposes of tracking, analysis and reporting. We will not otherwise disclose your personal data outside the ResearchGate or the Springer Nature group of companies unless we have your permission as detailed in the Privacy Policy.
While Users may use the Springer Nature journal content for small scale, personal non-commercial use, it is important to note that Users may not:

1. use such content for the purpose of providing other users with access on a regular or large scale basis or as a means to circumvent access control;
2. use such content where to do so would be considered a criminal or statutory offence in any jurisdiction, or gives rise to civil liability, or is otherwise unlawful;
3. falsely or misleadingly imply or suggest endorsement, approval , sponsorship, or association unless explicitly agreed to by Springer Nature in writing;
4. use bots or other automated methods to access the content or redirect messages
5. override any security feature or exclusionary protocol; or
6. share the content in order to create substitute for Springer Nature products or services or a systematic database of Springer Nature journal content.

In line with the restriction against commercial use, Springer Nature does not permit the creation of a product or service that creates revenue, royalties, rent or income from our content or its inclusion as part of a paid for service or for other commercial gain. Springer Nature journal content cannot be used for inter-library loans and librarians may not upload Springer Nature journal content on a large scale into their, or any other, institutional repository.
These terms of use are reviewed regularly and may be amended at any time. Springer Nature is not obligated to publish any information or content on this website and may remove it or features or functionality at our sole discretion, at any time with or without notice. Springer Nature may revoke this licence to you at any time and remove access to any copies of the Springer Nature journal content which have been saved.
To the fullest extent permitted by law, Springer Nature makes no warranties, representations or guarantees to Users, either express or implied with respect to the Springer nature journal content and all parties disclaim and waive any implied warranties or warranties imposed by law, including merchantability or fitness for any particular purpose.
Please note that these rights do not automatically extend to content, data or other material published by Springer Nature that may be licensed from third parties.
If you would like to use or distribute our Springer Nature journal content to a wider audience or on a regular basis or in any other manner not expressly permitted by these Terms, please contact Springer Nature at

onlineservice@springernature.com